IEEE Access
Multidisciplinary | Rapid Review | Open Access Journal

Received April 19, 2021, accepted May 3, 2021, date of publication May 10, 2021, date of current version May 25, 2021.

Digital Object Identifier 10.1109/ACCESS.2021.3078821

A Study on Accurate Initial Rotor Position Offset Detection for a Permanent Magnet Synchronous Motor Under a No-Load Condition

DONGOK KIM, JUNGJUN KIM, HEESUN LIM, JIHWAN PARK, JUNSEO HAN, AND GEUNHO LEE

Department of Automotive Engineering, Kookmin University, Seoul 02707, South Korea

Corresponding author: Geunho Lee (motor@kookmin.ac.kr)

This work was partly supported by the National Research Foundation of Korea (NRF) grant funded by the Korea government (Ministry of Science and ICT) (Innovative Incubation Center for Autonomous xEV Technology) (No. 5199990814084).

ABSTRACT This paper proposes a resolver offset calibration algorithm that can detect offset with high precision just by configuring a very simple experimental environment. This use of a simple experimental environment holds a great advantage for large-capacity permanent magnet synchronous motors (PMSMs) that require substantial resources to configure an experimental environment, such as EV traction motors. The proposed algorithm is designed based on the PMSM voltage equation. The algorithm is first verified for its validity through simulation with Simulink. Subsequently, it is implemented based on the C-language and installed on an inverter for verification experiments. The implemented algorithm is very simple and requires little execution time and memory. The error in the calibrated offset is experimentally found to converge within 3-bits based on 12-bits (the resolution of the commonly used RDC), and the results have very little deviation.

INDEX TERMS Permanent magnet synchronous motor (PMSM), IPMSM, permanent magnet motor, rotor initial position, offset angle, resolver offset.

I. INTRODUCTION

Recently, permanent magnet synchronous motors (PMSMs) have been widely adopted in automotive applications due to such advantages as small size, high efficiency, and easy control. To control these motors with high performance, techniques such as vector control are widely used [1]–[5]. To accomplish vector control of a PMSM, there are two required conditions to produce electromagnetic torque proportional to the q-axis current in the synchronously rotating frame aligned with the rotor position. First, the correct rotor position must be known for the park and inverse park variable transformations. Second, the d-axis current in the same rotating reference frame must be controlled to zero [6]–[7].

It is necessary to detect accurate rotor position information for coordinate transformation to satisfy both conditions. In general, position sensors such as encoders, MR sensors and resolvers are mainly used to detect the rotor's precise position information [8]. In particular, resolvers are primarily used in automotive applications. When using a resolver, the electric angle resolution is determined regardless of the number of poles of the motor, so even a multipole motor can minimize the electric angle error due to the initial rotor position. However, in the position sensor described, an offset error inevitably occurs in the rotor position information due to imbalance caused by product characteristics such as assembly tolerance between the motor and sensor, as shown in Fig. 1 [9]. The position offset of permanent magnet should be clearly identified for accurate torque control (less than 2%) and for suitable high-speed operation in the flux weakening region.

Inaccurate position information causes torque control errors as speed increases, making appropriate torque control impossible and resulting in poor efficiency and noise, vibration, and harshness (NVH) characteristics. In particular, the EV traction motor has a maximum speed specification equivalent to a maximum of 4 to 5 times the rated speed due to the system's characteristics to ensure controllability in the high-speed range, and an exact offset setting is required [10].

The associate editor coordinating the review of this manuscript and approving it for publication was Atif Iqbal.

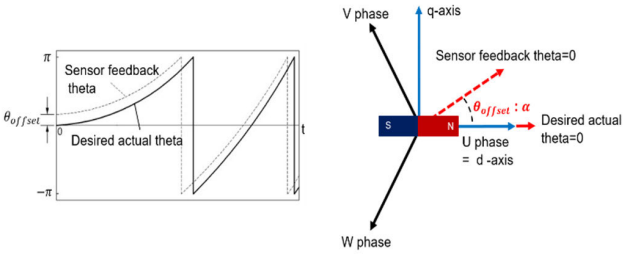

FIGURE 1. Electric angle of PMSM during rotating and offset angle in d-q axis coordinate system.

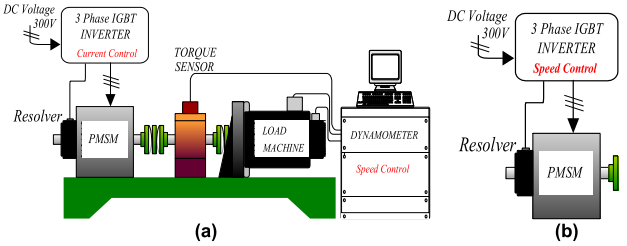

FIGURE 2. No load test setup (a) and dynamo test setup (b) to measure the rotor initial position offset.

The conventional rotor position offset detection method divides the problem into a load environment that requires external driving, such as a dynamo system and a no-load environment. First, because the position offset in the load condition in Fig. 2(a) uses the integral term of the d-axis current controller, a method for converging the output voltage of the d-axis to zero and a method of driving the motor in both directions were researched. In the case of using the d-axis current controller integral term, there is an advantage that it is possible to estimate the polarity of the rotor, but this requires an external driving environment such as a dynamo system, and there is a disadvantage in that there are errors due to the time delay and dead time of the power device. The control method of converging the d-axis current controller's output voltage to zero has the advantage that the rotor position can be estimated through a simple algorithm. Nevertheless, there is a disadvantage in that there are errors due to the controller's gain value and the dead time. Finally, the bidirectional driving method has the advantage of being able to estimate the initial position of the rotor more precisely than other methods through a simple algorithm that considers time delay [11], [12]. However, this method has the disadvantage that it requires an external infrastructure such as a dynamo system and is not suitable for EV traction motor mass production.

In the rotor's initial position detection method in the no-load environment of Fig. 2(b), there is a d-axis alignment after I/F drive [13], a d-q axis current measurement after d-axis alignment, and a high-frequency signal injection. The d-axis alignment method after I/F drive and the d-q current measurement method after d-axis alignment have the advantage of being able to estimate the initial position of the rotor in the no-load condition by a simple algorithm. However, this method has inferior initial rotor offset accuracy, and the deviation of the error is significant. The high-frequency signal injection method also has the advantage that it is possible to estimate the rotor position offset at standstill. In the case of high-frequency injection, however, signal processing such as DFT, BPF, or LPF is required to remove the high-frequency component of the current caused by a specific high-frequency signal to be injected. In the SPMSM or a motor with low salient polarity, the difference in inductance is not significant, so the high-frequency injection method's accuracy may decrease [14]–[18]. Moreover, when it is necessary to detect the resolver offset in a no-load state, such as mass production, the rotor may move slightly, and the precision may decrease.

In previous studies, the bidirectional drive method, which requires an external load environment, was found to enable the best initial rotor position estimation. However, substantial time consumption and cost were incurred to configure the load environment, requiring external driving. Therefore, in this study, we propose a new rotor initial position offset detection algorithm with high precision applied in a no-load environment that does not require an external driving system. In the no-load bidirectional driving method presented in this study, errors that may occur due to dead time or PWM time delay can be minimized and can provide precise initial rotor position offset estimation. These points make it easier to measure the motor's initial position than any other method. There is also the advantage of applicability not only to automotive applications but also in motor mass production.

II. NO-LOAD TWO-SPEED BIDIRECTIONAL ROTOR INITIAL POSITION DETECTION

A. ROTOR POSITION DETECTION WITH THE DYNAMO SYSTEM

The previous studies confirmed that the detection method of the load environment requiring dynamo system could accurately estimate the rotor initial position. In the bidirectional driving method using the dynamo system, the dynamo machine drives constantly the target PMSM forward and in reverse, and the target PMSM is controlled to zero current (the d- and q-axis currents are respectively zero). The rotor initial offset angle is calculated by the d- and q-axis voltages of the PMSM synchronous coordinate system using Equations (1)∼(5).

In Fig. 3(a), when there is an offset angle α, the d- and q-axis voltage equation is as shown in Equations (1) and (2) below.

$$V_d = (L_1 - L_2\cos 2\alpha)\frac{di_d}{dt} - L_2\sin 2\alpha\frac{di_q}{dt} - \omega_m\phi_f\sin\alpha + i_d(R_s + L_2\omega_m\sin 2\alpha) - i_q\omega_m(L_1 + L_2\cos 2\alpha) \quad (1)$$

$$V_q = (L_1 + L_2\cos 2\alpha)\frac{di_q}{dt} - L_2\sin 2\alpha\frac{di_d}{dt} + \omega_m\phi_f\cos\alpha + i_q(R_s - L_2\omega_m\sin 2\alpha) - i_d\omega_m(L_1 - L_2\cos 2\alpha) \quad (2)$$

where V_d, V_q, i_d, i_q are the synchronous rotating reference frame d-axis and q-axis voltages and currents and

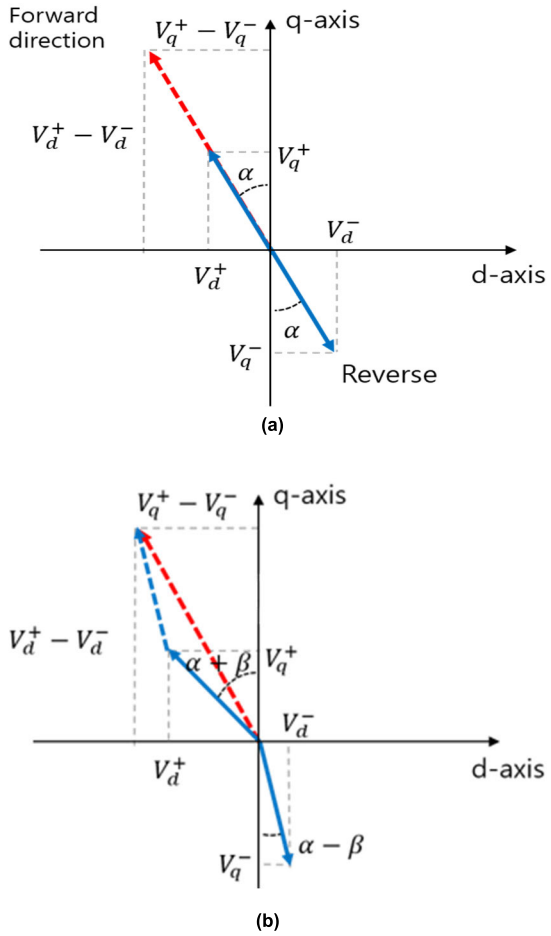

FIGURE 3. d, q voltage vector when the PMSM is driven forward and reversely with accurate electric angle (a) and time-delay electric angle offset (b).

$R_s, L_1, L_2, \omega_m, \phi_f$ are the stator resistance, inductances ($L_d = L_1 - L_2, L_q = L_1 + L_2$), rotor speed and magnetic flux, respectively.

If the d- and q-axis currents are controlled to zero, Equations (1) and (2) are expressed in Equations (3) and (4).

$$V_d^+ = -\omega_m \phi_f \sin\alpha \tag{3}$$
$$V_q^+ = \omega_m \phi_f \cos\alpha \tag{4}$$

However, when the motor is driven, the time delay component β is generated in the offset angle. To consider the time delay, the motor compensates for the voltage equation after driving in the reverse direction at the same speed as the forward speed, as shown in Fig. 3(b). When driving in both directions, the final offset angle is obtained, as shown in Equation (5).

$$\alpha + \beta = \tan^{-1}\left(\frac{V_d^+ - V_d^-}{V_q^+ - V_q^-}\right) \tag{5}$$

where $V_d^+, V_q^+, V_d^-, V_q^-$ are the d- and q-axis voltages operating forward and in reverse.

B. ANALYSIS OF THE TWO-SPEED BIDIRECTIONAL METHOD UNDER NO LOAD

Bidirectional rotor position offset detection using the dynamo system is a very accurate method, but is very expensive, takes a long time and is inconvenient in mass production. Therefore, a no-load environmental method that does not require dynamo system is needed.

The method must be able to detect the accurate rotor initial position when the PMSM is self-driven at speed control.

The q-axis current for constant speed control generates the voltage drop and dead time effect associated with insulated gate bipolar transistors (IGBTs), resulting in poor accuracy in the initial position detection.

To eliminate the dead time effect and the switching device voltage drop, this paper adopts the voltage difference method between the speed ω_{m2} and speed ω_{m1} when the PMSM is self-driven under no load.

In this case, the synchronous rotating reference frame d- and q-axis voltage vectors are expressed as shown in Fig. 4.

With the initial position of the rotor set to α' found by the d-axis alignment method after the I/F drive, only the q-axis current that controls the speed of the target motor is applied. The voltage equation can be summarized as Equations (6) and (7) as follows:

$$V_d = -\omega_m \phi_f \sin\alpha'' - i_q \omega_m (L_1 + L_2 \cos 2\alpha'') \tag{6}$$
$$V_q = \omega_m \phi_f \cos\alpha'' + i_q (R_s - L_2 \omega_m \sin 2\alpha'') \tag{7}$$

where α'' is the offset correction angle to be obtained by the bidirectional driven method.

When the PMSM is driven in the forward direction at speed ω_m^+, the voltage equation can be written as the following Equations (8) and (9) considering the switching device voltage drop and the dead time effect voltage.

$$V_d^+ = -\omega_m^+ \phi_f \sin\alpha'' - i_q^+ \omega_m^+ (L_1 + L_2 \cos 2\alpha'') + V_d^{CE} + V_d^{DT} \tag{8}$$
$$V_q^+ = \omega_m^+ \phi_f \sin\alpha'' + i_q^+ (R_s + L_2 \omega_m^+ \sin 2\alpha'') + V_q^{CE} + V_q^{DT} \tag{9}$$

where $V_d^{CE}, V_q^{CE}, V_d^{DT}, V_q^{DT}$ are the d- and q-axis voltage drops by the switching device (IGBT), representing the dead time effect voltage. When the PMSM is driven reversely at speed ω_m^-, the voltage equations of synchronous rotating frame can be written as the following Equations (10) and (11).

$$V_d^- = -\omega_m^- \phi_f \sin\alpha'' - i_q^- \omega_m^- (L_1 + L_2 \cos 2\alpha'') - V_d^{CE} - V_d^{DT} \tag{10}$$
$$V_q^- = \omega_m^- \phi_f \sin\alpha'' + i_q^- (R_s + L_2 \omega_m^- \sin 2\alpha'') - V_q^{CE} - V_q^{DT} \tag{11}$$

Since it is a no-load environment and the speed fluctuation $\Delta\omega_m(\omega_{m2} - \omega_{m1})$ is small, Δi_q of the q-axis current is negligible even if the speed increases.

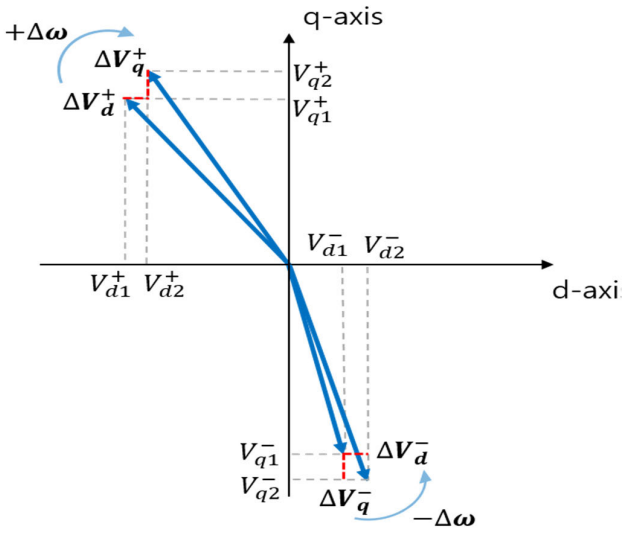

FIGURE 4. d, q voltage vector of two speeds during the two-speed bidirectional method.

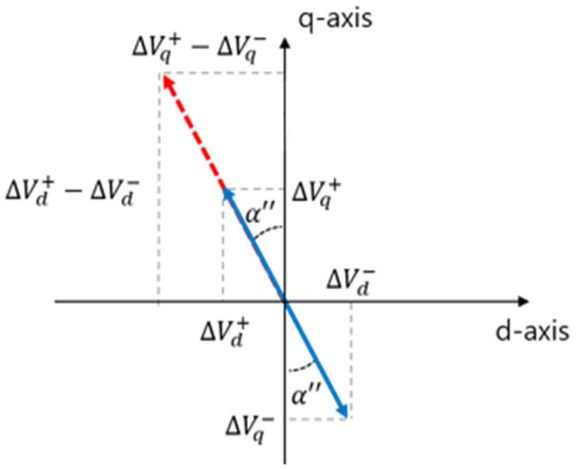

FIGURE 5. Two-speed voltage difference during no-load two-speed bidirectional drive offset angle.

Therefore, it is assumed that the dead time voltage and voltage drop (V_d^{CE}, V_q^{CE}) associated with the switching device (IGBT) are the same regardless of the speed.

The d- and q-axis voltage equations under the two-speed bidirectional method is summarized are as shown in Equations (12), (13), (14), and (15).

$$\Delta V_d^+ = V_d^{+\omega_{m2}} - V_d^{+\omega_{m1}} = -\Delta\omega_m^+\phi_f \sin\alpha'' - \Delta i_q^+ \Delta\omega_m^+ (L_1 + L_2 \cos 2\alpha'') \quad (12)$$

$$\Delta V_q^+ = V_q^{+\omega_{m2}} - V_q^{+\omega_{m1}} = \Delta\omega_m^+\phi_f \cos\alpha'' + \Delta i_q^+ (R_s - L_2 \Delta\omega_m^+ \sin 2\alpha'') \quad (13)$$

$$\Delta V_d^- = -\Delta\omega_m^-\phi_f \sin\alpha'' - \Delta i_q^- \Delta\omega_m^- (L_1 + L_2 \cos 2\alpha'') \quad (14)$$

$$\Delta V_q^- = \Delta\omega_m^-\phi_f \cos\alpha'' + \Delta i_q^- (R_s - L_2 \Delta\omega_m^- \sin 2\alpha'') \quad (15)$$

The difference between the forward q-axis voltage and reverse q-axis voltage ($\Delta V_d^+ - \Delta V_d^-, \Delta V_q^+ - \Delta V_q^-$) is calculated as Equations (16) and (17), assuming $\Delta\omega_m^+ = -\Delta\omega_m^-$, $\Delta i_q^+ = -\Delta i_q^-$,

$$\Delta V_d^+ - \Delta V_d^- = -2\Delta\omega\phi_f \sin\alpha'' \quad (16)$$

$$\Delta V_q^+ - \Delta V_q^- = 2\Delta\omega\phi_f \cos\alpha'' + 2\Delta i_q R_s \quad (17)$$

$$\Delta V_q^+ - \Delta V_q^- = 2\Delta\omega\phi_f \cos\alpha'' \quad (17\text{-}1)$$

Δi_q is negligible because it is very small at no load, so the voltage equation (Equation (17)) can be rewritten as Equations (17-1). Therefore, the offset correction angle α'' to be found by the two-speed bidirectional driven method is as shown in Equation (18) and Fig. 5.

$$\alpha'' = \tan^{-1}\left(\frac{\Delta V_d^+ - \Delta V_d^-}{\Delta V_q^+ - \Delta V_q^-}\right) \quad (18)$$

C. ENHANCED ROTOR POSITION OFFSET DETECTION USING THE PMSM DRIVER ONLY

In this study, a speed bidirectional method is proposed for the rotor initial position under no load as shown in Figs. 4 and 5.

The PMSM driver executes to find the rotor initial position at the no-load condition in the mass production. The target PMSM, which needs to find the rotor initial position, should be self-driven at the constant speed control with the PMSM driver. The voltage drop component and dead time effect of motor driver can be eliminated by increasing the target motor speed at regular intervals. First, to execute the speed control of the target PMSM, it is necessary to obtain the approximate initial rotor offset angle by driving the PMSM I/F and aligning the rotor to the d-axis, as shown in the flow chart on the left side of Figure 6.

To align the rotor to the d-axis, first, the electric angle (θ) that is used in vector control is set to 0, and then the current is applied to the d-axis.

If the current applied to the d-axis is not large enough, the rotor cannot be appropriately aligned to the d-axis. In contrast, if the current is too large, the electric angle is restricted to 0, so direct current flows undesirably in the system. In this study, a current that corresponds to approximately 50–70% of the motor's rated current is applied. With current applied to the d-axis, an electric angle with a frequency of 10 Hz is then created and driven by I/F. When driving at a deficient speed up to 0.5 Hz while lowering the frequency, the electrical angle (θ) is constrained toward a value of 0 again with $0 < \theta < \frac{2\pi}{5}$. At this time, the electric angle read from the position sensor is selected as an offset angle for the target motor speed control. Second, speed control must be performed on the target motor for a no-load bidirectional drive. The speed at which the target motor is controlled has to do with voltage accuracy and minimum current drive. In this study, voltage accuracy is crucial because the initial rotation angle is estimated using the d- and q-axis voltages.

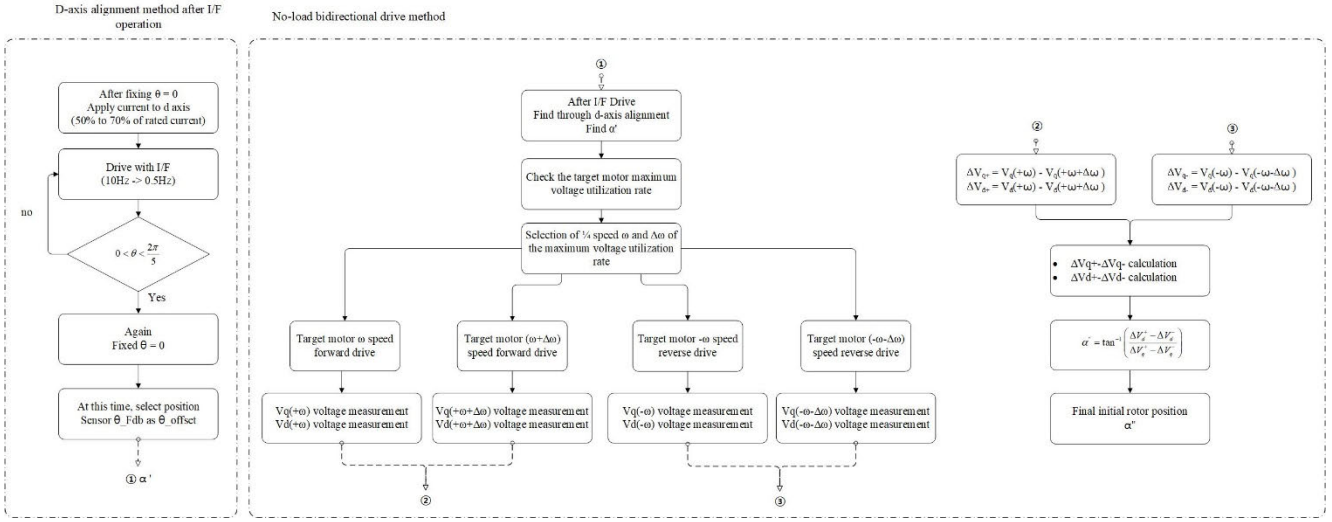

FIGURE 6. No-load, two speed, bidirectional drive method flow chart.

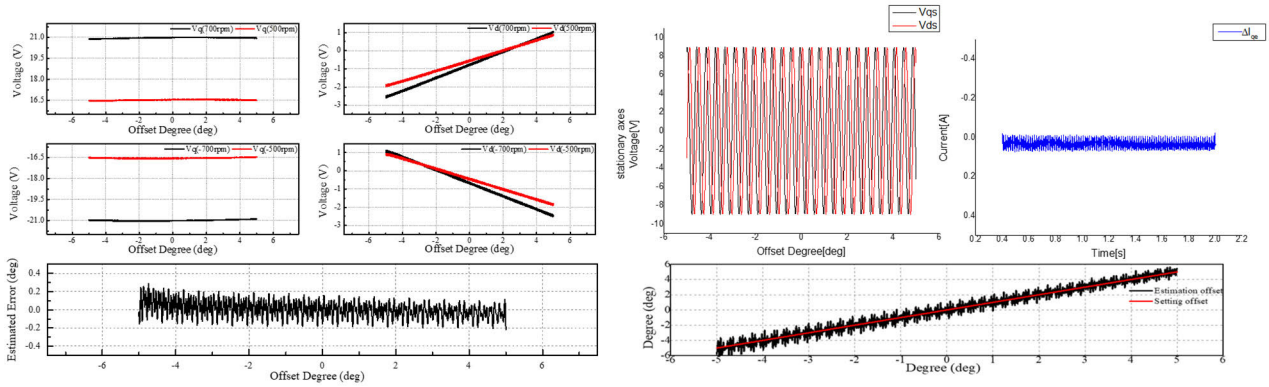

FIGURE 7. No-load, two speed, bidirectional drive method simulation.

Depending on the target motor, the speed control range is set at approximately 1/4 of the voltage utilization ratio. In addition, the less current is applied, the better the accuracy, so the measurement was performed at a low speed.

At speeds that are less than 1/4 of the voltage utilization ratio, the speed control performance is degraded, and the voltage accuracy is lowered due to instability in the voltage output. Because the target motor controls the speed, the q-axis current component is created. The voltage drop and dead time effect of the switching device due to the q-axis current occurs. To remove the collector emitter voltage drop associated with IGBTs and the dead time effect, the speed of the target motor is increased at a constant interval $\Delta\omega_m(\omega_{m2} - \omega_{m1})$, and ΔV_d^+, ΔV_q^+ can be obtained by measuring the d and q-axis voltages at each time. $\Delta\omega_m(\omega_{m2} - \omega_{m1})$ was determined in consideration of the voltage loss. In Equation (17), the larger the velocity interval, the larger Δi_q becomes, so the voltage drop component also grows. In this study, the above speed interval was selected as the maximum value to limit the voltage drop to less than 2% of the rated voltage. When driving in the reverse direction, ΔV_d^-, ΔV_q^- can be obtained in the same way.

Simulations were conducted using MATLAB Simulink to verify the no-load bidirectional driving algorithm presented in Fig. 7. In this study, simulations were conducted by selecting an 8 kW class integrated starter and generator (ISG), which are essential for eco-friendly cars. The specifications of the motor are shown in Tables 1 and 2. The speed control range was conducted at approximately 500–700 rpm, which is 1/4 of the motor's maximum voltage utilization rate. The simulation changed the offset of the position sensor from $-5.5°$ to $+5.5°$ to verify that the actual electric angle offset angle was estimated using the algorithm suggested in this study whenever the electric angle offset changed. In addition, in Equation (18), the components of $\Delta V_q^+ - \Delta V_q^-$ and $\Delta V_d^+ - \Delta V_d^-$ are shown in the stationary axes of the coordinate system. It was confirmed that Δi_q in Equation (17), which was generated by the application of this algorithm, is negligible and very small. As a result of the simulation, it was confirmed that the electric angle offset was estimated within $\pm 0.2°$.

TABLE 1. Specification of the 8 kW ISG and 100 kW traction motor (Ioniq Hybrid system of Hyundai Motors Co).

Property	8 kW	100 kW
Phase resistance [Ω]	0.124	0.0272
The d-axis inductance [mH]	1.034	0.147
The q-axis inductance [mH]	3.039	0.266
Magnetic flux [mVs/rad]	70.9	66.1
Poles	6	8

TABLE 2. Dimensions of 8 Kw ISG.

Property	8 kW
Stator outer diameter	128 mm
Rotor outer diameter	72 mm
Stack length	80 mm
Mechanical air-gap	0.5 mm

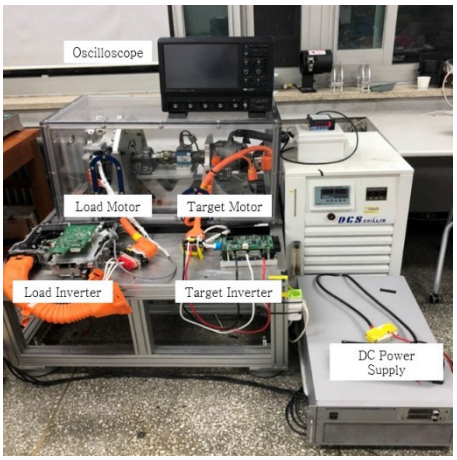

FIGURE 8. Experimental setup with dynamo system.

The most significant advantage of this method is that the electric angle offset can be obtained most accurately by the methods for detecting the rotor's initial position in a no-load environment. Moreover, the algorithm is much simpler than the high-frequency signal injection method.

III. EXPERIMENTAL RESULTS OF THE TWO-SPEED BIDIRECTIONAL ROTOR INITIAL POSITION DETECTION

A. EXPERIMENTAL SETUP

In this section, the existing rotor initial position detection methods and the two speeds bidirectional driven method are compared. We constructed a dynamo system with an 8 kW ISG for the hybrid system of Hyundai Motors Co. and a 100 kW traction motor (load motor of the dynamo system), as shown in Fig. 8. Both motors use a resolver as a position sensor and are universally applied to eco-friendly vehicles.

The ISG and traction motor are interior-type PMSMs. The specifications of the PMSM are shown in Table 1 and Table 2. Fig. 9 shows the magnetic flux density distribution of the ISG motor.

Before the experiment, the two-speed bidirectional position detection method assumes that the q-axis current

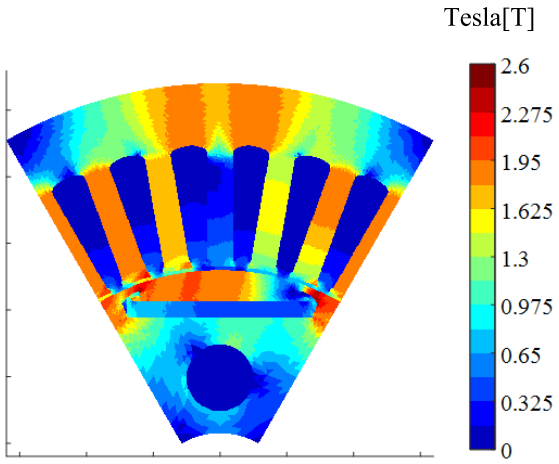

FIGURE 9. Flux density distribution of 8 Kw ISG at load condition.

magnitude fluctuation according to the speed is negligible. When the motor is driven under no load, back EMF E is generated by the rotor magnetic flux and motor speed. At the time of speed control at $\Delta\omega$ intervals, the change in the counter electromotive force by $\Delta\omega$ causes the current change by Δi. Since it is in a no-load state, a change in the back EMF by $\Delta\omega$ requires a minimal amount of current by Δi, as shown in the phasor diagram of Fig. 10. We confirmed experimentally that the difference in the q-axis currents ($\Delta I_q^+ = I_q^{+\omega_{m2}} - I_q^{+\omega_{m1}}$) is small during speed control at no load, as shown in Fig.10. When the ISG motor is driven to a constant speed by the dynamo system, the synchronous rotating frame voltage V_q of the ISG controller according to speed is monitored, as shown in Fig. 11 (digital-to-analog output of the MCU).

B. COMPARISON OF THE EXPERIMENTAL RESULTS

In the test, a 14-bit resolution resolver to a digital converter is used, and position detection is performed every 100 μs. The rotor position is precisely tuned by EMF measurements and the pure d-axis measuring method using the dynamo system. In the pure d-axis measuring method, the dynamo load system is driven under speed control mode, and the target 8 kW ISG motor is driven under current control mode ($I_q = 0, I_d =$ rated d-axis current). Then, we can manually tune the accurate rotor position offset that generates the zero torque output. When the 100 kW traction PMSM is tested, the 8 kW ISG motor is driven under speed control mode as the dynamo system.

Several rotor initial position estimation algorithms are performed repeatedly (10 times) for the 8 kW ISG motor and 100 kW traction motor. Test results are shown in Figs. 12 and 13. Fig. 14 shows the mean error and standard deviation.

The experiments confirm that the bidirectional driven method (at the load condition with the dynamo system) provides higher precision than the two-speed bidirectional driven method (among the alternate algorithms tested), with an average electric angle error of 0.166° for the 8 kW ISG motor

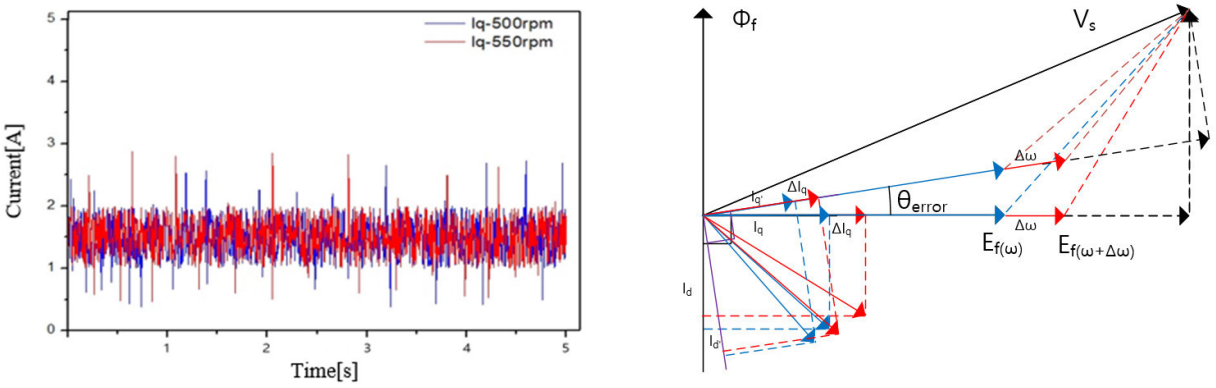

FIGURE 10. Comparison of q-axis current at no load (500 and 550 rpm) and phasor diagram.

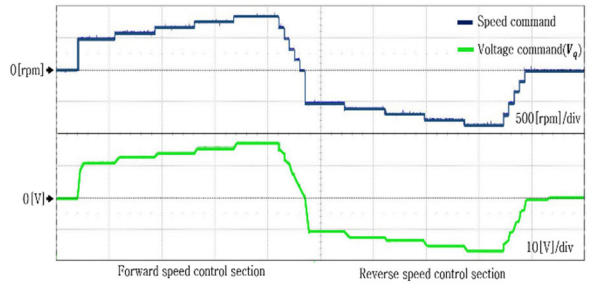

FIGURE 11. V_q voltage with the no-load, bidirectional method according to speed.

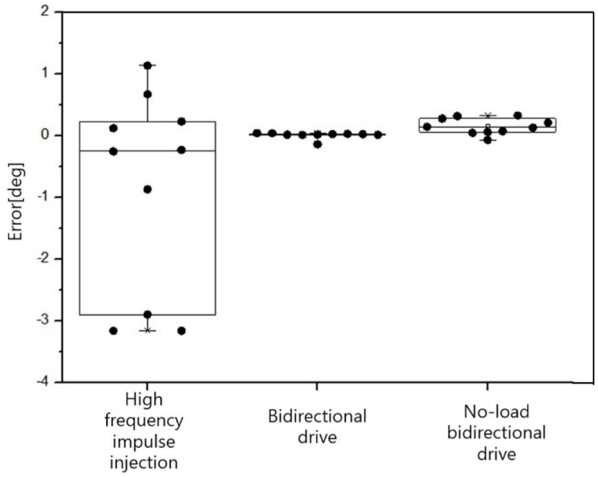

FIGURE 12. Comparison of rotor position estimation results (8 kW ISG Motor).

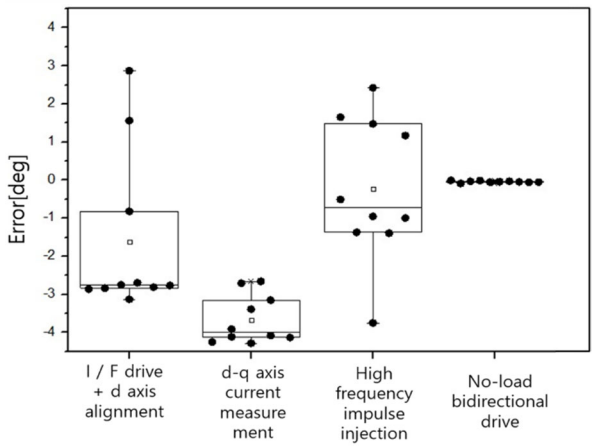

FIGURE 13. Comparison of rotor position estimation results (100 Kw traction motor).

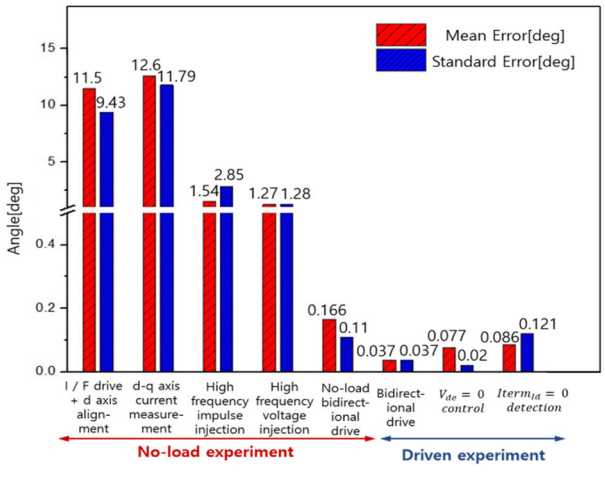

FIGURE 14. Test results of several methods (8kW ISG motor).

and an average electric angle error of 0.041° for the 100kW traction motor. However, as indicated by the experimental results, the rotor's initial position can be estimated within 0.3 deg of the mean error. A resolver with a 4095 pulse resolution used in the experiment can be estimated within three pulses (approximately 0.264 deg). It can be seen that it has sufficient accuracy to be applied to actual motor mass production.

In the 100 Kw traction motor, the high-frequency injection method has an error of 1.569°. The two-speed bidirectional method under the no-load condition can detect more than 70% more accurately than the high-frequency signal injection method. Therefore, it was verified that the proposed algorithm has sufficient accuracy to be applied in the motor mass production process, as shown in Fig. 12–Fig. 15.

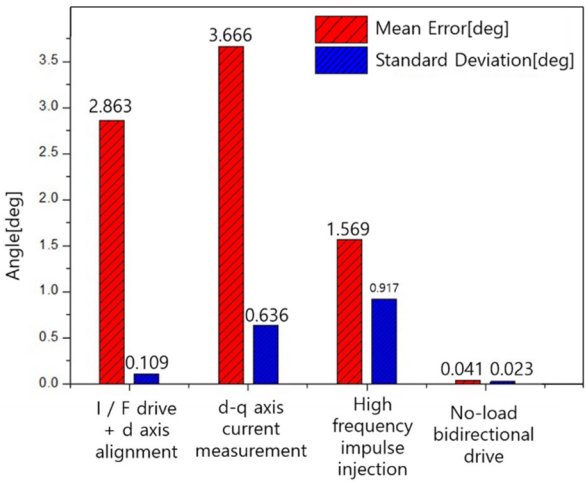

FIGURE 15. Experimental results of several methods for no-load condition (100 Kw traction Motor).

TABLE 3. No-load bidirectional rotor position detection according to the current sensor resolution.

Property	Mean Error [°]	Standard Deviation [°]
50 A Current Sensor	0.041	0.023
400 A Current Sensor	0.054	0.025

TABLE 4. No-load two-speed bidirectional rotor position detection according to the speed.

Rpm	Mean Error [°]	Standard Deviation [°]
±100 ~±300	0.032	0.023
±300 ~±500	0.106	0.072
±500 ~±700	0.038	0.036
±700 ~±900	0.037	0.039

Furthermore, we compared the variation in the current control accuracy according to the current sensor resolution (which can affect the estimation accuracy) and the variation according to the test speed. A comparison was made between the use of a current sensor that detects up to 400 A and 50 A. The test results are shown in Table 3, confirming that the accuracy of current control according to the current sensor does not significantly affect the accuracy of the algorithm.

Next, the speed control effect was divided into four ranges—100–300 rpm, 300–500 rpm, 500–700 rpm, and 700–900 rpm, as shown in Table 4, and repeated ten times to compare the application of the no-load, two-speed, bidirectional driven method. It can be verified that there is little difference in accuracy with varying test speed. Therefore, it can be confirmed that the no-load two-speed bidirectional driven algorithm presented in this study is robust against the current control accuracy and test speed of the target motor.

IV. CONCLUSION

In this study, first, we compared and analyzed the existing rotor initial position detection methods, proposed a simple and accurate rotor initial position detection algorithm, and verified this algorithm by experiments. The proposed method to detect the rotor initial position under a no-load environment is based on the bidirectional driven method, which has the highest accuracy at the forced driven environment using the dynamo system.

Two motors with different specifications were tested to verify the initial rotor position estimation algorithm proposed in this study. The high-frequency signal injection method, which is the most accurate method of detecting the initial position of the rotor in the existing no-load environment, had an average error of approximately 1°.

However, note that the frequency and current amplitude of the signal injection method must be selected according to the PMSM characteristics, such as saliency. On the other hand, the proposed no-load two-speed bidirectional driven method had average error within 0.3°, with low standard deviation. It was confirmed that the performance was very good compared to that of the existing method. The proposed no-load, two-speed, bidirectional driven method has the advantage that it is simple, requires no additional test equipment, and offers a very powerful capability for mass production. Finally, the initial position of the rotor can be estimated with only current control and speed control by the PMSM driver itself.

REFERENCES

[1] G. Boztas and O. Aydogmus, "Design of a high-speed PMSM for flywheel systems," in *Proc. 4th Int. Conf. Power Electron. Appl. (ICPEA)*, Sep. 2019, pp. 1–5.

[2] N. Murali, S. Ushakumari, and V. P. Mini, "Performance comparison between different rotor configurations of PMSM for EV application," in *Proc. IEEE REGION 10th Conf. (TENCON)*, Nov. 2020, pp. 1334–1339.

[3] G. Pellegrino, A. Vagati, P. Guglielmi, and B. Boazzo, "Performance comparison between surface-mounted and interior PM motor drives for electric vehicle application," *IEEE Trans. Ind. Electron.*, vol. 59, no. 2, pp. 803–811, Feb. 2012.

[4] D. D. Popa, L. M. Kreindler, R. Giuclea, and A. Sarca, "A novel method for PM synchronous machine rotor position detection," in *Proc. Eur. Conf. Power Electron. Appl.*, 2007, pp. 1–10.

[5] S. Sakunthala, R. Kiranmayi, and P. N. Mandadi, "A study on industrial motor drives: Comparison and applications of PMSM and BLDC motor drives," in *Proc. Int. Conf. Energy, Commun., Data Analytics Soft Comput. (ICECDS)*, Aug. 2017, pp. 537–540.

[6] S. Bai and E. W. Zhang, "Based on the model of the DQ axis permanent magnet synchronous motor MPC," in *Proc. Int. Conf. Electron. Optoelectron.*, Jul. 2011, pp. V3-224–V3-226.

[7] R. C. Garcia and J. O. P. Pinto, "Angular position control of permanent magnet synchronous motor using compensation of the nonlinearities of the DQ-model," in *Proc. IEEE 25th Int. Conf. Electron., Electr. Eng. Comput. (INTERCON)*, Aug. 2018, pp. 1–4.

[8] D. Lu, J. Gu, J. Li, M. Ouyang, and Y. Ma, "High-performance control of PMSM based on a new forecast algorithm with only low-resolution position sensor," in *Proc. IEEE Vehicle Power Propuls. Conf.*, Sep. 2009, pp. 1440–1444.

[9] C. W. Secrest, J. S. Pointer, M. R. Buehner, and R. D. Lorenz, "Improving position sensor accuracy through spatial harmonic decoupling, and sensor scaling, offset, and orthogonality correction using self-commissioning MRAS methods," *IEEE Trans. Ind. Appl.*, vol. 51, no. 6, pp. 4492–4504, Nov. 2015.

[10] K.-Y. Cho, Y.-K. Lee, H.-S. Mok, H.-W. Kim, B.-H. Jun, and Y.-H. Cho, "Torque ripple reduction of a PM synchronous motor for electric power steering using a low resolution position sensor," *J. Power Electron.*, vol. 10, no. 6, pp. 709–716, Nov. 2010.

[11] J. S. Bang and T. S. Kim, "Automatic calibration of a resolver offset of permanent magnet synchronous motors for hybrid electric vehicles," in *Proc. Amer. Control Conf. (ACC)*, Jul. 2015, pp. 4174–4179.

[12] J.-Y. Park, Y.-K. Ko, D.-Y. Jang, M.-S. Kwak, and Y.-K. Lee, "Auto calibration of position sensor while driving ECO vehicle," in *Proc. IEEE Transp. Electrific. Conf. Expo, Asia–Pacific (ITEC Asia–Pacific)*, Jun. 2016, pp. 397–401.
[13] M. Fatu, R. Teodorescu, I. Boldea, G.-D. Andreescu, and F. Blaabjerg, "I-F starting method with smooth transition to EMF based motion-sensorless vector control of PM synchronous motor/generator," in *Proc. IEEE Power Electron. Spec. Conf.*, Jun. 2008, pp. 1481–1487.
[14] H.-D. Kang, S.-H. Hwang, and J. Lee, "Initial rotor position estimation of single-phase permanent magnet synchronous motor with asymmetric air-gap," in *Proc. IEEE Transp. Electrific. Conf. Expo, Asia–Pacific (ITEC Asia–Pacific)*, Jun. 2018, pp. 1–5.
[15] L. M. Gong and Z. Q. Zhu, "Robust initial rotor position estimation of permanent-magnet brushless AC machines with carrier-signal-injection-based sensorless control," *IEEE Trans. Ind. Appl.*, vol. 49, no. 6, pp. 2602–2609, Nov. 2013.
[16] S. Medjmadj, D. Diallo, C. Delpha, and G. Yao, "A salient-pole PMSM position and speed estimation at standstill and low speed by a simplified HF injection method," in *Proc. IECON-43rd Annu. Conf. IEEE Ind. Electron. Soc.*, Oct. 2017, pp. 8317–8322.
[17] J. Liu, Y. Zhang, H. Yang, and W. Shen, "Position sensorless control of PMSM drives based on HF sinusoidal pulsating voltage injection," in *Proc. IEEE Energy Convers. Congr. Expo. (ECCE)*, Oct. 2020, pp. 3849–3853.
[18] B. Yuanjun, G. Xinhua, S. Xiaofeng, W. Yanfeng, and C. Yin, "Initial rotor position estimation of PMSM based on high frequency signal injection," in *Proc. IEEE Conf. Expo Transp. Electrific. Asia–Pacific (ITEC Asia–Pacific)*, Aug. 2014, pp. 1–4.

DONGOK KIM received the B.S. degree in mechatronics engineering from Korea Polytechnic University, Gyeonggi-do, Republic of Korea, in 2016, and the master's degree in automotive engineering from Kookmin University, Seoul, Republic of Korea, in 2018, where he is currently pursuing the Ph.D. degree in automotive engineering. His research interests include power conversion devices and permanent magnet ac motor control.

JUNGJUN KIM received the B.S. and M.S. degrees in automotive engineering from Kookmin University, Seoul, Republic of Korea, in 2018 and 2020, respectively. In 2020, he joined the LG Innotek Motor Control Research and Development Institute, where he develops motor control and an inverter systems for R-EPS.

HEESUN LIM received the B.S. degree in mechanical and automotive engineering, Kookmin University, Seoul, Republic of Korea, in 2015. She has been attended the integrated master's and doctoral program with the Kookmin University's Graduate School of Automotive Engineering, since 2016. Her current research interests include the advanced control of electric machines and automotive inverters.

JIHWAN PARK received the M.S. degree in automotive engineering from Kookmin University, Seoul, South Korea, in 2019, where he is currently pursuing the Ph.D. degree in automotive engineering. His current research interests include the advanced control of electric machines and automotive inverters.

JUNSEO HAN received the B.S. degree in electronic engineering from Inha University, Incheon, Republic of Korea, in 2019, and the master's degree in automotive engineering from Kookmin University, Seoul, Republic of Korea, in 2021, where he is currently pursuing the Ph.D. degree in automotive engineering. His research interests include electronic machines, sensorless motor control, and their applicable nonlinear control for improvement in control performance

GEUNHO LEE received the B.S. and M.S. degrees in electrical engineering and the Ph.D. degree in automotive engineering from Hanyang University, Seoul, South Korea, in 1992, 1994, and 2010, respectively. From 1994 to 2002, he was with the LG Industrial Research Institute, where he developed inverter systems for elevators. Since 2011, he has been a Professor in automotive engineering with Kookmin University. His current research interests include electric vehicles and the advanced control of electric machines.